www.cadanda.com
Computer-Aided Design AND APPLICATIONS

Efficient Bolus Shaping for Cancer Care

Zohreh Sohrabi Ghareh Tappeh [1] and Qingjin Peng[2]

[1]University of Manitoba, sohrabiz@myumanitoba.ca
[2]University of Manitoba, Qingjin.Peng@umanitoba.ca

Corresponding author: Qingjin Peng, Qingjin.Peng@umanitoba.ca

Abstract. Bolus is used to cover patient skin in radiation therapy of cancer care to improve the dose delivery. The existing method of bolus shaping is a manual process that is time-consuming and inaccurate. This paper introduces a process to improve the accuracy of bolus shaping and fabrication efficiency using an unfolding-folding method. Three main operations are investigated for mesh simplification, unfolding and folding processes, and accuracy evaluation of fabricated models. The process of simplifying 3D models is discussed using different simplification algorithms to evaluate quality of solutions. The simplified models are unfolded to generate 2D patterns that are then cut into material pieces to be folded back to 3D shape. Case studies show that the accuracy of fabricated 3D prototypes meets the bolus requirement.

Keywords: 3D modeling, Mesh simplification, Unfolding, Design and evaluation, Software tool.
DOI: https://doi.org/10.14733/cadaps.2022.587-601

1 INTRODUCTION

In radiation therapy, a tissue-equivalent bolus material is used to conform closely to the target area of patient skin to enhance dose delivery. The bolus should cover the skin perfectly [3,5]. However, for some irregular surfaces such as elbow, nose, and knee, airgaps may be generated between the bolus and patient skin. The airgaps will reduce dose delivery to the patient skin and affect treatment quality. The current method used for bolus shaping in cancer care is a manual process based on trial and error which is time-consuming and inaccurate. Usually, airgaps bigger than 5 mm will result in incomplete treatment. Although 3D printing methods have been introduced in bolus shaping with improved accuracy, there is no daily clinical experience with customized 3D printed bolus [4]. Time-consuming process and limited materials are main limitations of 3D printing techniques. In this paper, a process is introduced to improve the accuracy of bolus shaping and fabrication efficiency using an unfolding-folding method which is one of the most prevalent techniques for 3D object fabrication from planar sheets [21].

With the advancement of technologies, especially in geometry acquisition devices such as 3D scanners, complex polygonal meshes with millions of vertices can be generated. Although real-

world objects can be modeled by these technologies, different levels of details are required for different applications. 3D models with complexity in shapes are difficulty in process [23,9]. It is necessary to develop robust and efficient mesh simplification techniques for eliminating redundant geometry of meshes for a trade-off between accuracy and efficiency. Research on the mesh simplification has received increasing attention. There are different simplification techniques of mesh models [20] such as follows. 1) Vertex clustering techniques as the dominant method simplify mesh models without an iterative process [14], 2) Vertex decimation techniques [15] iteratively operate candidate vertices for eliminating the loop of triangles around selected vertex, and re-triangulating the hole [8,16], and 3) Iterative edge contraction techniques use iterative operators. Full-edge collapse, half-edge collapse, and vertex-per collapse operators are applied in this method. In addition, isotropic surface remeshing is another approach to simplify high-density triangular surfaces uniformly. The instant field-aligned meshes approach [7] works based on a local smoothing operator and sharp features control.

The unfolding and folding process has been introduced as an alternative and cost-saving solution for creating 3D objects from planar materials [22]. Unwrapping a 3D mesh model into 2D surfaces is called unfolding. The flattened pattern is then cut and folded back into a 3D shape. A minimum number of generated 2D patches, quality of the flattened patterns [10], and automation of unfolding algorithm are three main criteria to measure the quality of mesh approximation algorithms. Processing time is another important factor in the unfolding and folding process. Minimizing the number of patches is important to reduce crafting time. A strip-based approximation method [19] can produce different foldable strips from simplified triangles. 19 different heuristic methods were studied [12] for unfolding 3D models to a net without overlapping edges. Steepest edge unfolding is one of the most effective approaches shown in the study. A convex polyhedron was flattened in a 100% success rate. In addition, self-overlaps problem on the flattened patches was studied in this research, however, a large volume of patches was generated. Our research searches an effective method for a trade-off between accuracy and efficiency in the unfolding-folding process.

2 METHODOLOGY

A method of 3D bolus fabrication is proposed to minimize airgaps between the bolus and patient skin. Three main operations are investigated for the mesh simplification, unfolding and folding processes, and accuracy evaluation of fabricated models as follows. 1) A simplification process is performed for 3D patient data to remove redundant information and then evaluated based on its reference model to ensure accuracy. 2) The simplified mesh model is flattened into 2D patches in an unfolding process. 3) 2D patches are cut from the bolus sheet material and folded back to the 3D shape which is then analyzed for accuracy compared to its original model. The process flow is shown in Figure 1. Details are as follows.

2.1 Simplification Process

A simplification process of the 3D mesh model is performed for the minimum information in unfolding and folding processes. Three widely used simplification and remeshing techniques, Clustering Decimation (CD), Quadric Edge Collapse Decimation (QECD) [11], and Instant Field-Aligned (IFA) [6, 7], are evaluated to find a proper technique for this process. The 3D mesh model is simplified in different reduction rates for evaluation compared to original models. Outputs of the three techniques are then compared in visual and computational aspects. For the computation comparison, Hausdorff Distance (HD) is measured to compare simplified and original models.

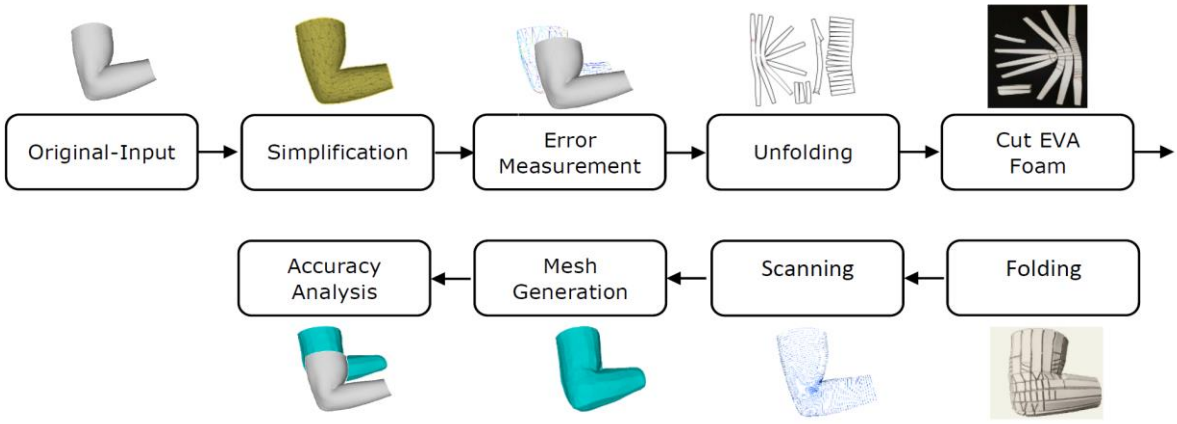

Figure 1: Flowchart of the proposed method.

The HD between two point-sets, M1 and M2, is defined as follows.

$$d_h(M_1, M_2) = \max_{a \in M_1} \min_{b \in M_2} \|a - b\| \tag{1}$$

Since the one-sided HD is non-symmetric, d_H(M1, M2) is defined as the maximum HD of two sides of a surface as follows.

$$d_H(M_1, M_2) = \max\{d_h(M_1, M_2), d_h(M_2, M_1)\} \tag{2}$$

The maximum and Root Mean Square (RMS) distances are used to find the largest generated distance as well as overall distances from the original model.

2.2 Unfolding Process

The simplified model using a proper simplification technique is flattened into 2D patterns. Three common unfolding software tools, Pepakura Designer [13], SketchUp [18], and Blender [2] with different algorithms, are investigated to find the most appropriate one to meet the bolus forming requirement. The unfolding algorithm of Blender tool uses edges with shorter lengths as well as steeper and concave angles for high priority of cut lines. All faces are cut and then joined to create a bigger patch based on edge preference. In case of overlapping, the cutting operation stops and moves to the next edge. In Pepakura Designer, faces of the mesh model are connected or separated considering folding angles and areas of the face adjacent to edges, edges with sharper angles have a preference to flatten. SketchUp uses a randomized algorithm without any creating distortion to flatten the resulting set of faces. The unfolding process is performed in two ways, automatically and manually. A subdivision operation is also applied to unfolded patterns to smooth sharp edges. Generated 2D patches from each tool are then compared in the number of patches and quality.

2.3 Evaluation

Outputs of the unfolding step are evaluated in a folding process. The bolus is made from a uniform thickness sheet material used in radiation therapy to cover patient treatment areas. In this research, a 10 mm thick Ethylene-Vinyl Acetate (EVA) foam material is used to examine the folding process.

In generated flattened patterns, there are two types of creases, mountain folds (convex) and valley folds (concave). Type of the crease depends on the view side of shape. Figure 2 shows creases with the mountain and valley folds on a zero-thickness sheet.

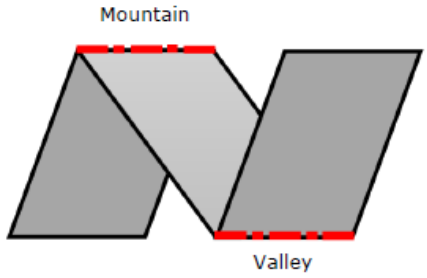

Figure 2: Mountain and valley folds.

As the material used in this study has 10 mm thickness, all creases in flattened patterns should be assessed before cutting and folding since inner surfaces of the 3D model should remain smooth for perfect fitting to the original surface as shown in Figure 3. On the other hand, valley folds should be created from the inner surface of model, which leads to a jagged surface. So some calculations are required for the crease creation on a thick material.

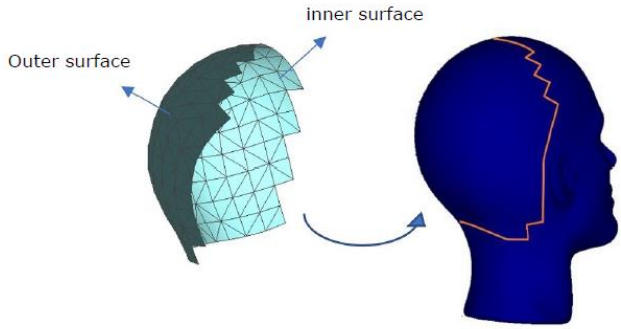

Figure 3: Fitting a 3D model to the target surface.

Figure 4 shows mountain and valley folds created on outer and inner surfaces of a thick material, respectively. As the inner surface is the target in this study, and creation of valley folds in the inner surface will result in distortion of the target surface, all creases with valley folds are created from the outer surface of the model by making a V-shaped groove. Creases with the mountain fold are created using a laser cutting machine as shown in Figure 5.

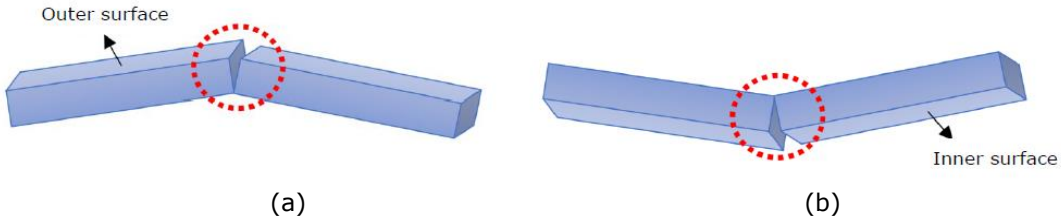

Figure 4: The mountain and valley on thick material, (a) crease with a mountain fold, (b) crease with a valley fold.

Figure 5: Performing semi-cut for creases with a mountain fold.

Creases with valley folds are then created for manipulation from outside surfaces of the model by making a V-shaped groove to keep the inner surface smooth as shown in Figure 6. The mathematical formulation of finding a V-shaped groove angle is shown in Eq.3, where β is the valley angle, and θ is an angle of the V-shaped groove which should be cut from each edge.

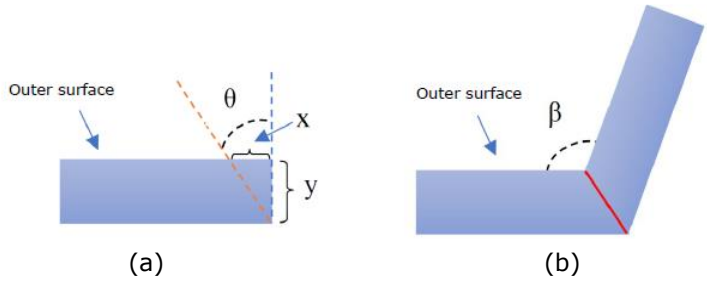

Figure 6: The angle cutting (V-shaped groove) for creases with a valley fold, (a) cutting angle and corresponding cutting length, (b) Attaching two edges for crease with a valley fold after cutting.

For simplicity in measuring and cutting angle θ, distance x shown in Figure 6(a) is calculated by Eq. 4. A cut is then made from point x along the hypotenuse (red line). A similar cut is made on the other edge of this valley and finally, the two edges are glued to create Figure 6(b).

$$\theta = 90 - \frac{\beta}{2} \tag{3}$$

$$\tan\theta = \frac{x}{y}, y = 10\ (mm), \qquad x = 10\tan\theta\ (mm) \tag{4}$$

Once the unfolded patterns are cut into patches, they are folded back into the 3D shape. Creases with mountain folds remain in 2D patterns to be formed by the laser cutter. Due to the thickness of EVA foam, semi-cuts are created for mountain folds on the outer surface as shown in Figure 5. In the folding process, angle of the mountain crease is set using an angle finder and the gap between the two edges is filled using hot glue as shown in Figure 7.

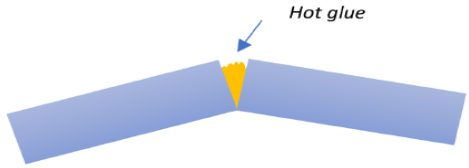

Figure 7: A crease with the mountain fold created using hot glue.

Creases with valley folds are created manually using V-shaped groove tools based on Figure 6 and Eqs. 3 and 4. The valley fold is then created using glue. Once the creases are created, angles of boundaries between patches are set using the angle finder and then glued all together.

Accuracy of the formed prototype is then evaluated by comparing its scanned data with its original 3D model. The prototype is first scanned using a 3D laser scanner to form a surface model of the prototype. A surface mesh model of the prototype is then generated using a software tool (Meshlab). The model is finally evaluated for the accuracy analysis.

3 CASE STUDIES

Two case studies are first utilized to apply and evaluate the proposed method by performing three simplification techniques (CD, QECD, and IFA). Three different simplified models are flattened into 2D patterns using different unfolding tools. Assessments are then carried out to choose the most appropriate solution.

3.1 Simplification Process

Two 3D models, a Face and Leg models, with different complexities, are imported into Meshlab and Instant Meshes as shown in Figure 8. A complicated face model (with 223987 triangles and 112862 vertices), and a moderate leg model (with 25173 triangles and 12891 vertices) are processed in six different decimation rates (60%, 70%, 80%, 90%, 99%, and 99.5%) to show performances of the simplification algorithm.

(a) (b)

Figure 8: Two 3D models used in the simplification process, (a) Face model, (b) Leg model.

Due to the large volume of triangles, both two simplified mesh models show a negligible difference from original models. Outputs of the simplification process for the face and leg models are shown in Figure 9.

It is shown that for both models, although meshes boundaries in QECD are fixed same as the original model, the model is destroyed in high reduction rates. On the other hand, in the CD method, the mesh boundary is not well preserved after simplification, and details of the model are also almost spoiled. However, using the IFA algorithm has a partial effect on details of the model.

To evaluate quality of simplified models obtained from the three algorithms, the HD is employed to measure the geometric difference between the simplified and original meshes. Plots of the maximum and RMS errors for all decimated models created by simplification algorithms are shown in Figure 10.

Error values are normalized with respect to the bounding box of the corresponding model to demonstrate relative errors. In the maximum error plots of both models, although QECD indicates the minimum difference between the simplified and original models in 60% to 90% reduction rates, by increasing the reduction level, errors are increased remarkably. The maximum value of

HD shows the biggest difference between the two mesh models, however, it is not the only factor for the evaluation of algorithms. Thus, the methods are also compared in RMS values. In RMS plots, errors of both models in QECD and IFA are lowest and highest, respectively.

3.2 Unfolding Process

In the unfolding process, three 3D mesh models, a part of an elbow, an eye with a tumor [1], and a nose are tested. Each model is first cut to separate the target area of the model and then simplified and re-meshed using QECD and IFA techniques provided in Meshlab and Instant Meshes, respectively. Figure 11 shows cases used in the unfolding process. The nose model with 127404 faces is simplified down to 258 and 255, using QECD and IFA techniques, respectively. Furthermore, elbow and tumor models with 26480 and 297255 faces are reduced to 408 and 230, respectively. Obtained models are then exported into three software tools, Pepakura Designer, Blender, and SketchUp, to convert into flattened 2D patterns, automatically and manually.

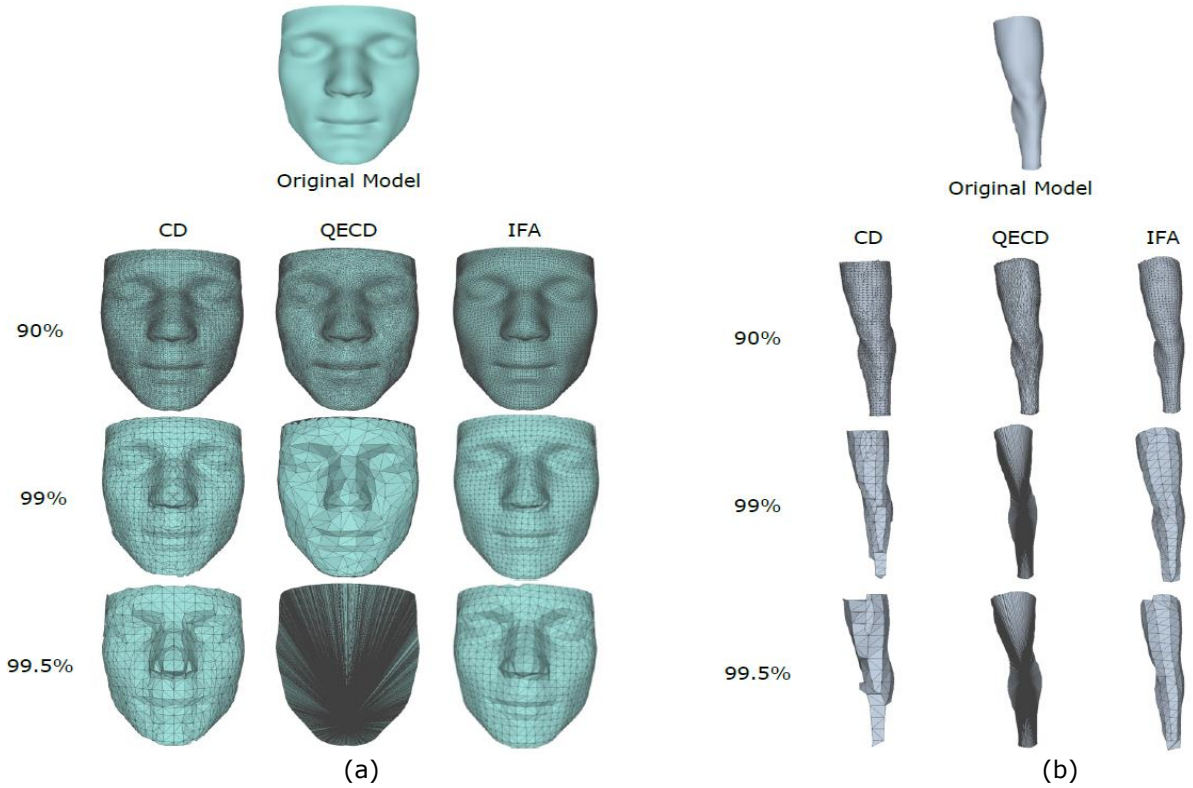

Figure 9: Sequence of decimation in 90%, 99%, and 99.5%, (a) Face model, (b) Leg model.

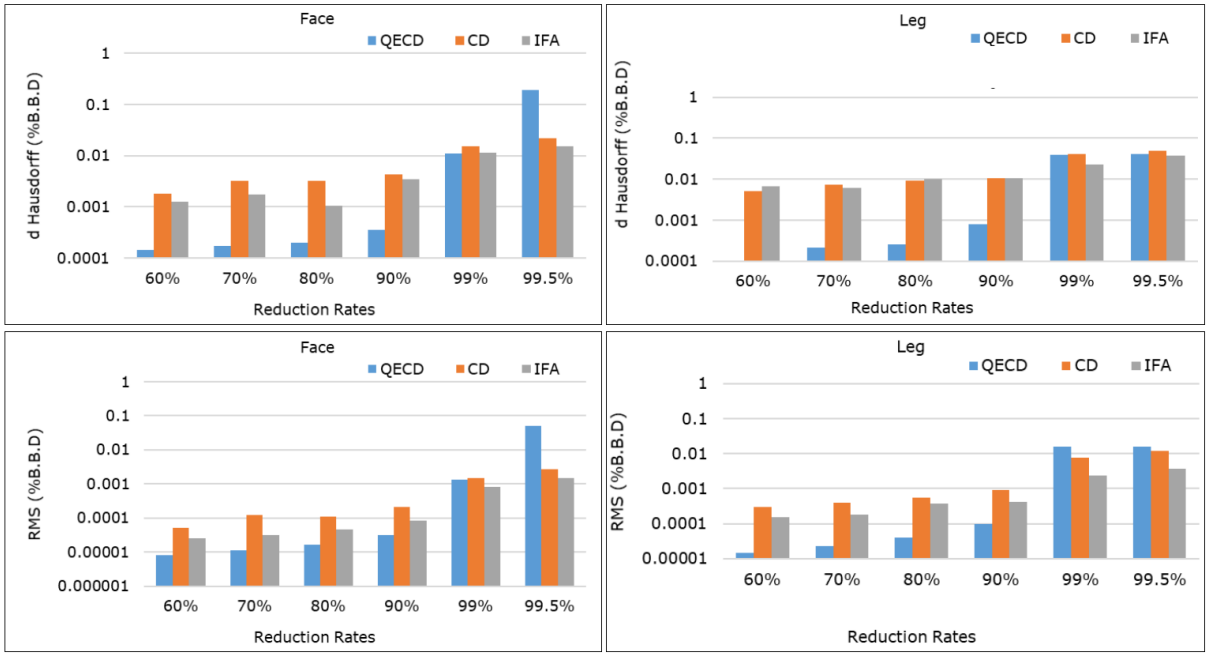

Figure 10: Maximum and RMS errors compared to the original models for all simplification implementations using HD for the face and leg models (B.B.D, Bounding Box Diagonal).

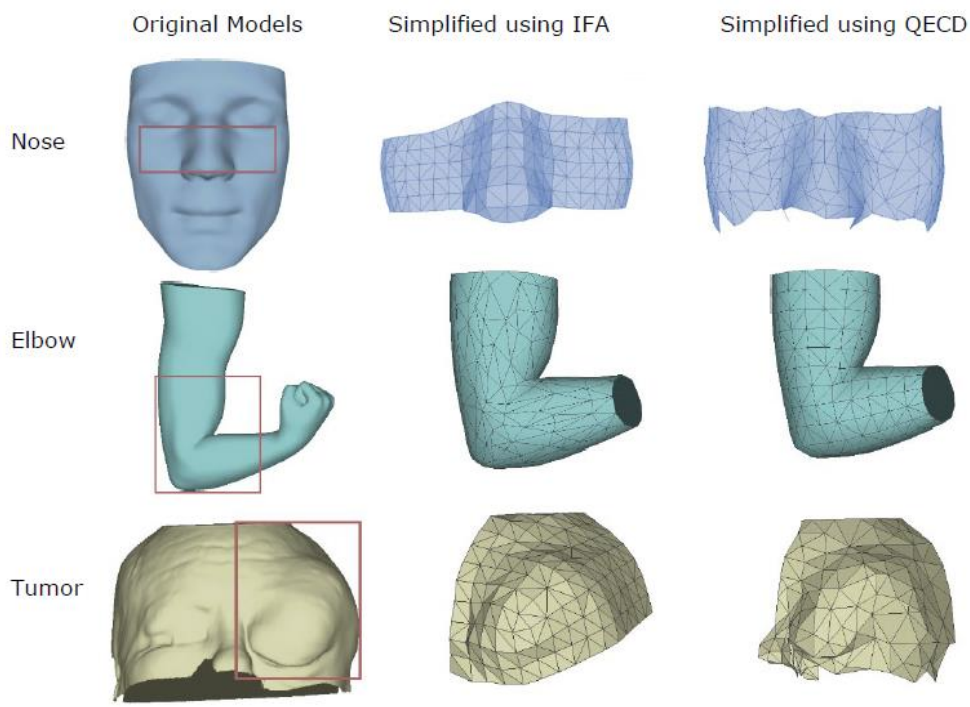

Figure 11: 3D models used in the unfolding-folding process.

Simplified versions of all the cases are first flattened in unfolding tools automatically. Figure 12 shows generated 2D patterns of the tumor model in Pepakura and Blender in an automatic process. As models used in this study are double-curved surfaces (not developable such as cylinders), it is found that SketchUp is incapable to unfold these models. On the other hand, Pepakura and Blender generate irregular 2D patterns with a large number of patches automatically. Moreover, it can be seen that IFA models are more regular due to the strip-based remeshing process in the Instant-Align Meshes tool and have less complexity compared to QECD models. Similar results are for other two models. Such a deformed pattern with lots of patches makes the folding process complicated and time-consuming. Therefore, simplified models are also analyzed in a manual unfolding process.

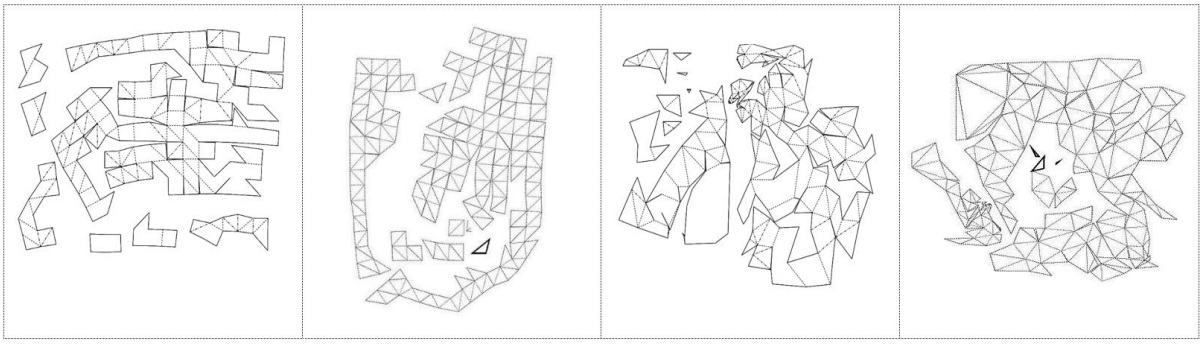

(a) (b) (c) (d)

Figure 12: Generated 2D patterns of simplified tumor models using IFA and QECD. (a, c) patterns in Pepakura Designer, (b, d) patterns in Blender.

Both Pepakura Designer and Blender provide manual function for the unfolding process. 2D patterns of the simplified tumor model made by the IFA technique in a manual unfolding process are shown in Figure 13. It can be seen that generated patterns in Pepakura Designer and Blender are the same in 3 patches. However, SketchUp generated 10 patches in a time-consuming process. In the manual unfolding process, patterns are generated in a strip triangle which is more regular than patterns in the automatic process. Furthermore, the number of patches is also reduced for the folding process in less time. Table 1 shows a summary of investigations of three unfolding tools.

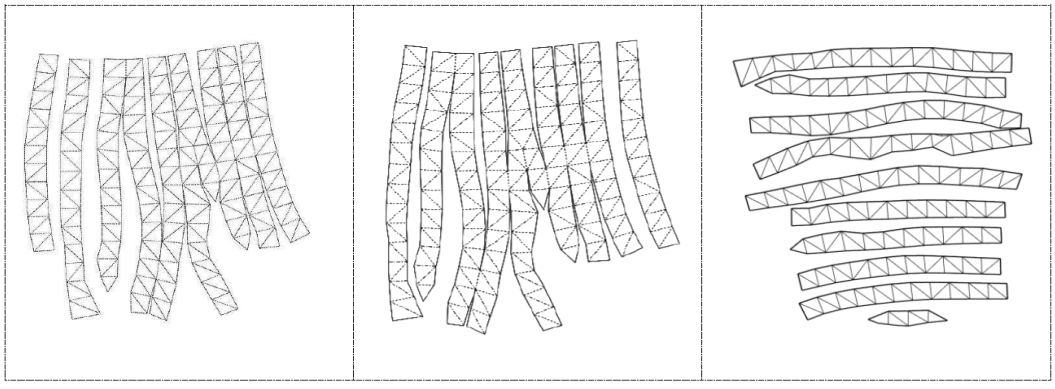

(a) (b) (c)

Figure 13: Manual strip-based unfolding of the tumor model, (a) 2D patterns in Pepakura, (b) 2D patterns in Blender, (c) 2D patterns in SketchUp.

Although results in using both tools are similar, there are some limitations in the Blender tool. At first, using Blender, generated 2D patterns are exported as a PDF format file and patterns cannot be shown and edited. Therefore, the model edition is based on trial and error that makes the process time-consuming. However, using Pepakura, patterns can be easily separated in case of overlapping faces or joined based on the user preference in a short time. Furthermore, Pepakura Designer exports the patterns in .PDO, .OBJ, and .DXF format files that are compatible with the laser cutting machine system.

Name of the Organ No. of Original faces Simplification method		Nose (127404 faces)		Elbow (26480 faces)		Tumor (297255 faces)	
		QECD	IFA	QECD	IFA	QECD	IFA
Simplification Data	Reduction(%)	99.8	99.8	98.5	98.5	99.9	99.9
	No. of faces	258	255	408	409	230	230
	HD (mm)	15.4	4.5	1.78	2.8	8.6	4.7
Unfolding (Auto) (No. of Patches)	Pepakura	11	9	3	4	9	7
	Blender	11	9	4	4	7	7
	SketchUp	-	-	-	-	-	-
Manual Unfolding (No.of Patches)	Pepakura	-	4	-	5	-	3
	Blender	-	4	-	8	-	3
	SketchUp	-	7	-	28	-	10
Manual Unfolding (Time (min))	Pepakura	-	1.2	-	3.8	-	2.6
	Blender	-	2.8	-	6.2	-	4.5
	SketchUp	-	4.3	-	15.5	-	6.8

Table 1: A summary of findings in the unfolding process.

A comparison of unfolding software tools is also shown in Table 2. In summary, the IFA technique is chosen as the simplification method for producing a uniform surface. Moreover, Pepakura Designer is also employed to generate 2D patterns of models based on triangle strips.

	Pepakura	Blender	SketchUp
Automated unfolding procedure	✓	✓	×
Mountain and valley angles	✓	×	×
Export to .DXF format	✓	×	✓
Editable pattern	✓	×	×

Table 2: Comparison of unfolding tools.

3.3 Evaluation

3.3.1 Model Fabrication and 3D shape folding

Based on analyzing 2D patterns generated in the unfolding process, it is found that simplified models using the IFA technique form strip patches make the folding process simple. On the other hand, the number of creases created in patches is too much to handle as shown in Figure 13. To

overcome this issue, those creases with angles very closed to 180 deg. are considered flat junctions. Therefore, it is decided to ignore creases with angles of more than 175 deg. Figure 14 shows that the number of creases in patterns of the elbow model is decreased considerably based on this assumption. The same results have been achieved for the nose and tumor models.

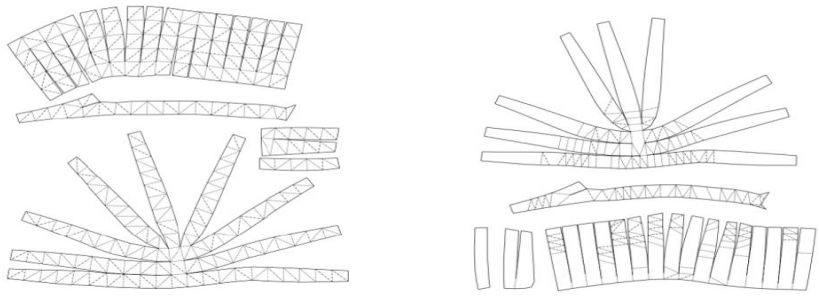

(a) (b)

Figure 14. Comparison of unfolded patterns of the elbow model, (a) pattern with entire creases, (b) pattern with creases in angles up to 175 degrees.

After creases assessment, generated 2D patterns are cut on an EVA foam sheet using a laser cutting machine. In the folding process, creases with mountain and valley folds in each patch are measured and created using the angle finder and hot glue, then patches of each model are glued together forming boundary edges (cut lines of each patch) to complete prototypes as shown in Figure 15.

(a) (b) (c)

Figure 15. Prototypes made from the EVA foam, (a) Nose, (b) Elbow, (c) Tumor.

The creation of each crease with mountain and valley folds takes 20 and 40 seconds. respectively. Moreover, each boundary edge with mountain and valley folds is created in 25 and 35 seconds, respectively. Table 3 shows the fabrication time of each model considering the number of creases.

The total fabrication time is also measured as an important factor of this study. To evaluate efficiency of the prototype fabrication, the processing time for each step is measured, separately. The time used for all the operations is shown in Table 4. It is indicated that the average time for model fabrication is less than 2 hours.

	Nose	Elbow	Tumor
No. of patches	4	5	3
No. of creases with a mountain fold	107	164	101
Creation Time(min)	36	55	34

No. of creases with a valley fold	33	9	11
Creation Time(min)	22	6	7.4
Boundary edges with a mountain fold	69	344	82
Creation Time(min)	7.2	35	8.6
Boundary edges with a valley fold	31	26	22
Creation Time(min)	18	15.2	12.9
Creation Time(min)	83.2	111.2	62.9

Table 3: Creation time of creases and boundary edges for fabricated prototypes.

Operation (min)	Nose	Elbow	Tumor
Simplification	8	15	7
Unfolding	5	10	8
Cutting	4	15	5
Folding	83.2	111.2	62.9
Total Time	100.2	151.2	82.9

Table 4: Fabrication time of the prototypes.

3.3.2 Model Measurement

Fabricated prototypes are measured using a ShapeGrabber 3D laser scanner available in the lab. The scanner has accuracy up to 0.01 mm [17]. The inner surface of each prototype is acquired as the target area with an average of 4 scans. Acquired scan data are exported into STL format files. The scan data are processed to reform models in Meshlab as shown in Figure 16.

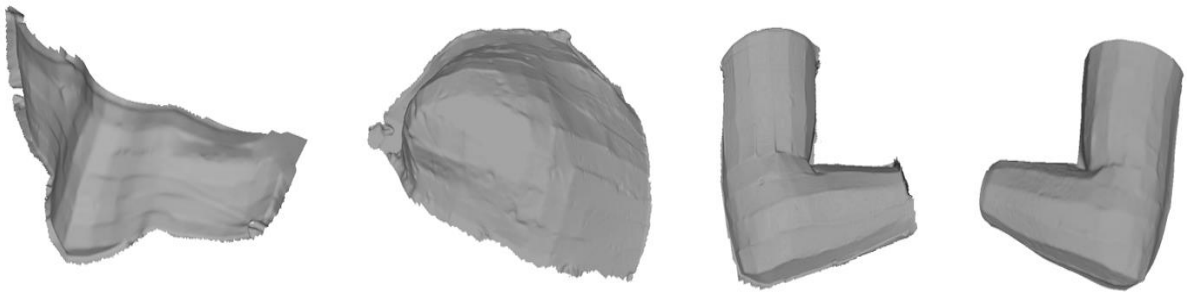

(a) (b) (c) (d)

Figure 16: Generated mesh models from fabricated prototypes using Meshlab, (a) Nose, (b) Tumor, (c)Elbow-Right, (d) Elbow-Left.

3.3.3 Accuracy Evaluation of Fabricated Prototypes

In the evaluation process, in order to find the accuracy of fabricated prototypes, a comparison between the original model and scanned prototype is performed. To do this, distances between the mesh data derived from the scanning process and the original CAD model are evaluated. For each model, the scanned prototype and original model are aligned together and then deviations between

the two models are measured. Geomagic Control X software tool is utilized to evaluate the fabricated prototypes as shown in Figures 17 and 18. Each model is evaluated with and without tolerance (green color shows the tolerance) to show the distances accurately. It is shown that for all three models, distances bigger than 5 mm occur only in boundary areas that are not our target and would be acceptable.

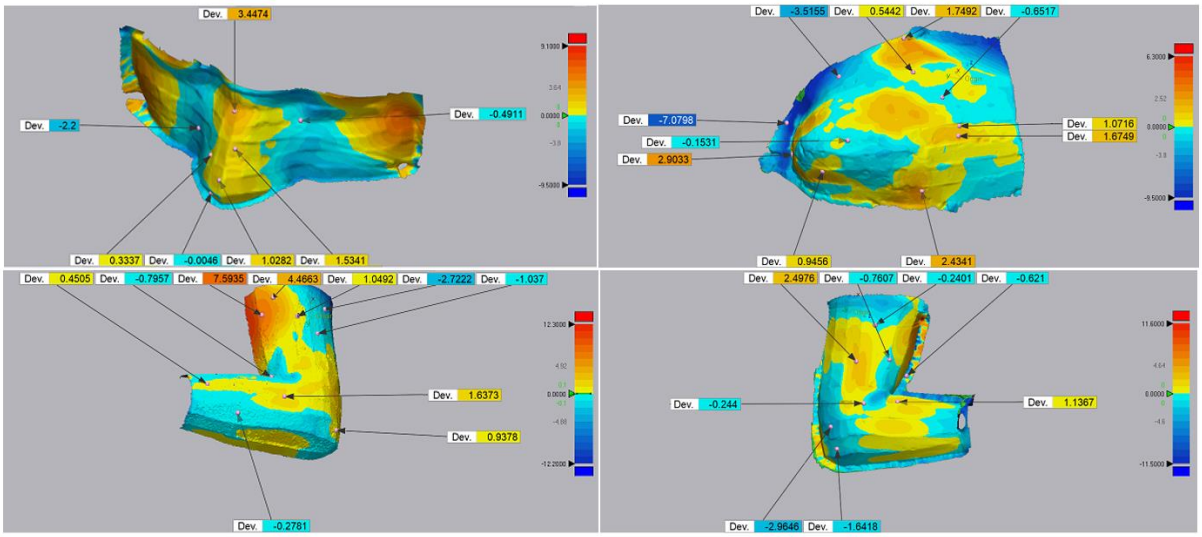

Figure 17: Deviation of the prototypes with their original models in Geomagic Control X without considering tolerance.

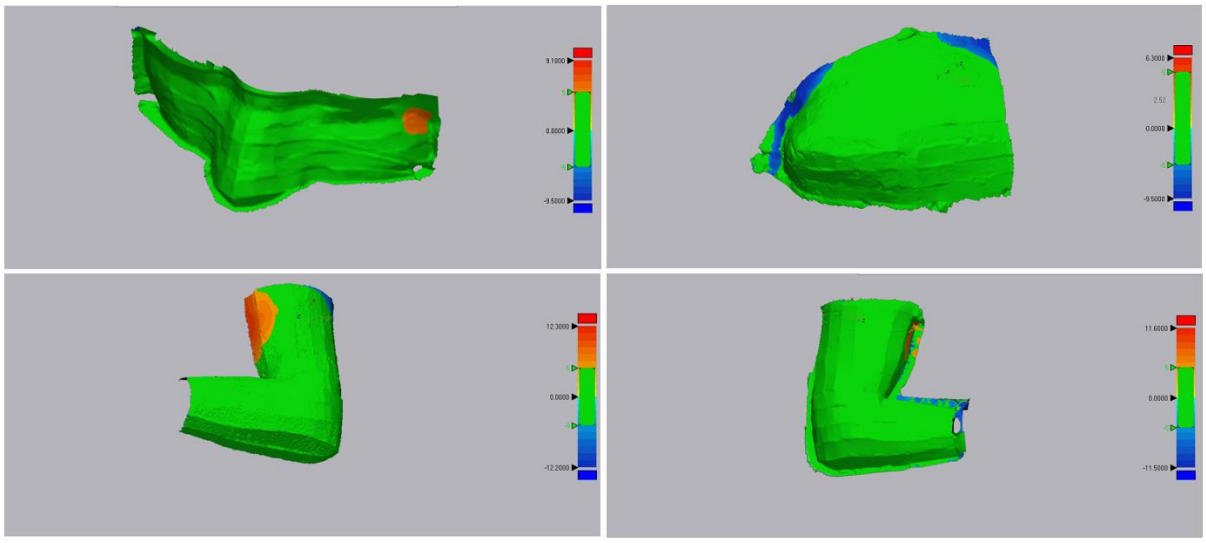

Figure 18: Deviation of the prototypes with their original models in Geomagic Control X considering the tolerance (green color).

4 CONCLUSION

In this paper, an unfolding and folding process is introduced as an alternative solution for 3D bolus shaping. Following solutions are concluded in this study. 1) In the model simplification process, the Instant Field-Aligned technique generates simplified mesh models with accurate and regular patterns. 2) In the unfolding process, Pepakura Designer provides expected functions to meet requirements of this study among investigated unfolding tools. On the other hand, unfolded patterns are generated based on trial and error in SketchUp resulted in a large number of patches. 3) The instant Field-Aligned model is unfolded in a regular pattern based on triangle strips, which makes the folding process easy. 4) The average total fabrication time is around 2 hours, which is considerably less than the time used by the 3D printing technique. 5) Results of the accuracy evaluation show that the deviation between the fabricated prototype and original model meets the requirement of this study. The further work will test the solution in clinic applications to improve the method.

ACKNOWLEDGMENTS

The authors wish to acknowledge that this research has been supported by the MITACS Accelerate program and Faculty of Graduate Studies. We would like to extend our sincere thanks to Dr. Harry Ingleby and Dr. David Sasaki in Cancer Care Manitoba for their suggestions and technical supports during this research.

Zohre Sohrabi Ghareh Tappeh, https://orcid.org/0000-0001-7260-0935
Qingjin Peng, http://orcid.org/0000-0002-9664-5326

REFERENCES

[1] 3D models, https://free3d.com/, Free 3D models.
[2] Blender, https:blender.org/, Blender software tool.
[3] Boone, M.-L; Almond, P.-R.; Wright, A.-E.: High-energy electron dose perturbations in regions of tissue heterogeneity, II. Physical models of tissue heterogeneities Radiology, vol. 88, no. 6, pp. 1146-53, 1967. https://doi.org/10.1148/88.6.1146
[4] Canters, R.-A.; Lips, I.-M.; Wendling, M.; Kusters, M.; Zeeland, M.-V.; Gerritsen, R.-M.; Poortmans, P.; Verhoef, C.-G.: Clinical implementation of 3d printing in the construction of patient specific bolus for electron beam radiotherapy for non-melanoma skin cancer, Radiotherapy and Oncology, vol. 121, no. 1, pp. 148-153, 2016. https://doi.org/10.1016/j.radonc.2016.07.011
[5] Chang, F.; Chang, P.; Benson, K.; Share, F.: Study of elasto-gel pads used as surface bolus material in high energy photon and electron therapy, Int J Radiat Oncol Biol Phys, vol. 22, no. 1, pp. 191-3, 1992. https://doi.org/10.1016/0360-3016(92)90999-x
[6] Instant Meshes, https://github.com/wjakob/instant-meshes, Instant Meshes tool.
[7] Jakob, W.; Panozzo, D.; Sorkine-Hornung, o.: Instant field-aligned meshes, ACM Transactions on Graphics, vol. 34, pp. 1-15, 10 2015. https://doi.org/10.1145/2816795.2818078
[8] Kobbelt, L.; Campagna, S.; Peter Seidel, H. : A general framework for mesh decimation, Proceedings of Graphics Interface, p. 43-50, 1998. https://doi.org/10.20380/GI1998.06
[9] Liu, X.; Lin, L.; Wu, J.; Wang, W.; Yin, B.; Wang, C.: Generating sparse self-supporting wireframe models for 3d printing using mesh simplification, graphical Models, vol. 98, p.14-23, 2015. https://doi.org/10.1016/j.gmod.2018.05.001
[10] Massarwi, F.; Gotsman, C.; Elber, G.: Paper-craft from 3D polygonal models using generalized cylinders, Computer Aided Geometric Design, vol. 25, p. 576-591, 2008. https://doi.org/10.1016/j.cagd.2008.06.007
[11] Meshlab, https://www.meshlab.net, Meshlab software.

[12] Nets of polyhedral, Schlickenrieder, Technical University of Berlin, 1997
[13] Pepakura Designer, https://tamasoft.co.jp/pepakura/index.html, Pepakura Designer software.
[14] Rossignac, J.; Borrel, P.: Multi-resolution 3d approximation for rendering complex scenes, p. 455-465, 1993. https://doi.org/10.1007/978-3-642-78114-8_29
[15] Schroeder, W.: A topology modifying progressive decimation algorithm, p. 205-212, 1997. https://doi.org/10.1109/VISUAL.1997.663883
[16] Schroeder, W.-J.; Zarge, J.-A.; Lorensen, W.-E.: Decimation of triangle meshes, SIGGRAPH Comput. Graph., vol. 26, p. 65-70, 1997. https://doi.org/10.1145/133994.134010
[17] ShapeGrabber, http://www.shapegrabber.com. ShapeGrabber 3D laser scanner.
[18] SketchUp, https://www.sketchup.com/, SketchUp software tool.
[19] Straub, R.; and Prautzsch, H.: Creating Optimized Cut-Out Sheets for Paper Models from Meshes, SIAM Conference on Geometric Design and Computing, vol. 2005, 2005. https://doi.org/10.5445/ir/1000012368
[20] Wang, Y.; Zheng, J.; Wang, H.: Fast simplification methods for three-dimensional geometric models with feature-preserving efficiency, Scientific Programming, vol. 2019, p. 1-12, 2019. https://doi.org/10.1155/2019/4926190
[21] Xi, Z.; Kim, Y.-H.; Kim. Y.-J.; Lien, J.-M.: Learning to segment and unfold polyhedral mesh from failures, Computers & Graphics, vol. 58, p. 139-149, 2016. https://doi.org/10.1016/j.cag.2016.05.022
[22] Xi, Z.; Lien, J.-M.; Continuous unfolding of polyhedra -ma motion planning approach, p. 3249-3254, 2015. https://doi.org/10.1109/IROS.2015.7353828
[23] Yuan, Y.; Wang, R.; Huang, J.; Jia, Y.; Bao, H.: Simplified and tessellated mesh for real-time high quality rendering, Computers & Graphics, vol. 54, p. 135-144, 2015. https://doi.org/10.1016/j.cag.2015.07.011